



## Bioactive norditerpenoids from the soft coral *Sinularia gyrosa*

Shi-Yie Cheng<sup>a,d</sup>, Cheng-Ta Chuang<sup>a</sup>, Zhi-Hong Wen<sup>a,d</sup>, Shang-Kwei Wang<sup>b</sup>, Shu-Fen Chiou<sup>a</sup>, Chi-Hsin Hsu<sup>a,d</sup>, Chang-Feng Dai<sup>c</sup>, Chang-Yih Duh<sup>a,d,\*</sup>

<sup>a</sup> Department of Marine Biotechnology and Resources, National Sun Yat-sen University, Kaohsiung 804, Taiwan

<sup>b</sup> Department of Microbiology, Kaohsiung Medical University, Kaohsiung 807, Taiwan

<sup>c</sup> Institute of Oceanography, National Taiwan University, Taipei, Taiwan

<sup>d</sup> Asia-Pacific Ocean Research Center, National Sun Yat-sen University, Kaohsiung 804, Taiwan

### ARTICLE INFO

#### Article history:

Received 8 February 2010

Revised 1 April 2010

Accepted 2 April 2010

Available online 8 April 2010

#### Keywords:

*Sinularia gyrosa*

Norcembranoids

Norditerpenoids

Anti-inflammatory activity

Cytotoxicity

Anti-HCMV (human cytomegalovirus)

Antibacterial activity

### ABSTRACT

Chemical investigations of the soft coral *Sinularia gyrosa* resulted in the isolation of six new norcembranolides, gyrosanolides A–F (**1–6**), a new norcembrane, gyrosanin A (**7**), and 11 known norditerpenoids **8–18**. The structures of the isolated compounds were elucidated through extensive spectroscopic data and by comparison with reported data in the literature. Compounds **1–3**, **7–9**, **12**, and **13** at concentration of 10  $\mu$ M did not inhibit the COX-2 protein expression, but significantly reduced the levels of the iNOS protein ( $55.2 \pm 14.6\%$ ,  $18.6 \pm 6.7\%$ ,  $10.6 \pm 4.6\%$ ,  $66.9 \pm 5.2\%$ ,  $10.2 \pm 5.1\%$ ,  $17.4 \pm 7.2\%$ ,  $47.2 \pm 11.9\%$ , and  $56.3 \pm 5.1\%$ , respectively) by LPS stimulation. Compound **8** showed significant antiviral activity against HCMV (human cytomegalovirus) cells with an  $IC_{50}$  of 1.9  $\mu$ g/mL.

© 2010 Elsevier Ltd. All rights reserved.

### 1. Introduction

Soft corals belonging to the genus *Sinularia* (Alcyoniidae) have proven to elaborate a rich harvest of unique C-4 norcembranoids and their derivatives.<sup>1–15</sup> A number of these macrocyclic norcembranoids were recently shown to exhibit an array of bioactivities such as anti-fungal<sup>6</sup> and cytotoxic properties.<sup>6,10–13</sup> The continuing search for bioactive constituents urged us to investigate the secondary metabolites of the soft coral *Sinularia gyrosa* (Tixier-Durivault, 1970), which was collected by hand using SCUBA along the coast of the Dongsha Atoll off Taiwan. We have succeeded in the isolation of seven new norcembranoids, gyrosanolides A–G (**1–7**), and 11 previously characterized norcembranoids **8–18**<sup>1,3,5,10–14</sup> from the acetone-soluble of the organism. The details of isolation and structural elucidation of these isolated norcembranoids are discussed. Compounds **1–6** and **8–18** were evaluated in vitro for cytotoxicity against P-388 (mouse lymphocytic leukemia), A-459 (human lung carcinoma), and HT-29 (human colon adenocarcinoma) cancer cell lines, antiviral activity against HCMV (human cytomegalovirus) cells, anti-inflammatory activity using RAW 264.7 macrophage cells, and antibacterial activity against five bacterial strains, comprising *Enterobacter aerogenes* (ATCC13048), *Salmonella enteritidis* (ATCC13076), *Serratia marcescens*

(ATCC25419), *Shigella sonnei* (ATCC11060), and *Yersinia enterocolitica* (ATCC23715).

### 2. Results and discussion

By a series of column chromatography using normal-phase silica and reversed-phase C<sub>18</sub> gel columns in combination with reversed-phase C<sub>18</sub> HPLC, the acetone extracts of the soft coral *S. gyrosa* resulted in the purification of six new norcembranolides, gyrosanolides A–F (**1–6**), a new norcembrane, gyrosanin A (**7**), and 11 known norditerpenoids **8–18** (see Section 3).

Gyrosanolide A (**1**) was obtained as a colorless oil. Its HRESIMS ( $m/z$  371.1472,  $[M+Na]^+$ ) and NMR spectroscopic data (Tables 1 and 2) established the molecular formula C<sub>19</sub>H<sub>24</sub>O<sub>6</sub>, implying the existence of eight degrees of unsaturation. The UV spectrum  $\lambda_{max}$  (MeOH) value at 223 nm together with the IR absorptions at 1734 and 1643 cm<sup>−1</sup> of **1** revealed the presence of a conjugated  $\gamma$ -lactone moiety, which was further indicated from the <sup>1</sup>H NMR signals at  $\delta_H$  6.43 (1H, dd,  $J = 12.0, 5.2$  Hz, H-13), 4.60 (1H, s, H-11), and 4.73 (1H, t,  $J = 3.6$  Hz, H-10) as well as <sup>13</sup>C NMR signals at  $\delta_C$  168.6 (qC, C-19), 131.8 (qC, C-12), 147.4 (CH, C-13), 71.4 (CH, C-11), and 83.0 (CH, C-10).<sup>12</sup> A strong IR spectrum absorptions at 1718 and <sup>13</sup>C NMR signals at  $\delta_C$  205.5 (qC, C-3) indicated the presence of a ketone functionality. In addition, the <sup>1</sup>H NMR signals at  $\delta_H$  6.39 (1H, s, H-7) and <sup>13</sup>C NMR signals at  $\delta_C$  200.5 (qC, C-6),

\* Corresponding author. Tel.: +886 7 5252000×5036; fax: +886 7 5255020.  
E-mail address: [yihduh@mail.nsysu.edu.tw](mailto:yihduh@mail.nsysu.edu.tw) (C.-Y. Duh).

**Table 1**<sup>1</sup>H NMR spectroscopic data of compounds **1–3**

H#	<b>1</b> <sup>a</sup>	<b>2</b> <sup>a</sup>	<b>3</b> <sup>a</sup>
1	3.09 m	3.03 m	2.97 m
2	1.96 m	a: 2.38 dd (16.8, 1.6) <sup>b</sup> ; b: 2.56 dd (16.8, 10.0)	2.27 m
4	a: 2.09 dd (16.8, 6.4) <sup>b</sup> b: 3.16 dd (16.8, 2.0)	a: 2.92 m b: 3.02 dd (17.6, 4.4)	a: 2.85 m b: 3.08 dd (16.0, 2.8) <sup>b</sup>
5	4.36 dd (6.0, 2.0)	4.29 t (4.0)	3.90 dd (7.6, 2.8)
7	6.39 s	6.15 s	6.66 s
9	a: 2.56 dd (13.6, 3.2) b: 2.87 dd (13.6, 3.6)	a: 2.48 dd (13.6, 1.6) b: 2.87 dd (13.6, 5.2)	a: 2.51 dd (14.0, 3.6) b: 2.88 m
10	4.73 t (3.6)	4.69 d (5.2)	4.70 t (3.6)
11	4.60 s	4.61 s	4.57 s
13	6.43 dd (12.0, 5.2)	6.64 dd (10.4, 6.4)	6.46 dd (11.6, 4.8)
14	a: 2.22 dt (13.6, 4.8) b: 3.53 td (13.6, 3.6)	a: 2.14 m b: 3.55 ddd (13.6, 10.4, 5.2)	a: 2.23 m b: 3.54 ddd (14.0, 11.6, 4.0)
16	a: 4.42 s; b: 4.85 s	a: 4.72 s; b: 4.82 s	a: 4.47 s; b: 4.85 s
17	1.82 s	1.78 s	1.79 s
18	2.33 d (0.8)	2.20 s	2.23 d (1.2)
5-OMe			3.41 s

<sup>a</sup> Spectra were measured in CDCl<sub>3</sub> (400 MHz).<sup>b</sup> *J* values (in Hz) are in parentheses.**Table 2**<sup>13</sup>C NMR spectroscopic data of compounds **1–7**

C#	<b>1</b> <sup>a</sup>	<b>2</b> <sup>a</sup>	<b>3</b> <sup>a</sup>	<b>4</b> <sup>b</sup>	<b>5</b> <sup>a</sup>	<b>6</b> <sup>a</sup>	<b>7</b> <sup>a</sup>
1	39.1 (CH) <sup>c</sup>	39.9 (CH) <sup>c</sup>	39.8 (CH) <sup>c</sup>	41.1 (CH) <sup>c</sup>	38.0 (CH) <sup>c</sup>	38.2 (CH) <sup>c</sup>	39.0 (CH) <sup>c</sup>
2	42.5 (CH <sub>2</sub> )	45.5 (CH <sub>2</sub> )	45.2 (CH <sub>2</sub> )	45.7 (CH <sub>2</sub> )	45.6 (CH <sub>2</sub> )	48.0 (CH <sub>2</sub> )	45.1 (CH <sub>2</sub> )
3	205.5 (qC)	205.4 (qC)	203.3 (qC)	206.9 (qC)	204.9 (qC)	208.3 (qC)	208.4 (qC)
4	47.4 (CH <sub>2</sub> )	47.0 (CH <sub>2</sub> )	45.1 (CH <sub>2</sub> )	48.1 (CH <sub>2</sub> )	45.1 (CH <sub>2</sub> )	44.3 (CH <sub>2</sub> )	43.5 (CH <sub>2</sub> )
5	74.1 (CH)	72.4 (CH)	82.4 (CH)	71.5 (CH)	76.4 (CH)	77.3 (CH)	75.4 (CH)
6	200.5 (qC)	200.4 (qC)	199.0 (qC)	200.1 (qC)	214.5 (qC)	211.4 (qC)	214.2 (qC)
7	124.2 (CH)	123.9 (CH)	124.0 (CH)	124.4 (CH)	49.4 (CH <sub>2</sub> )	51.0 (CH <sub>2</sub> )	44.2 (CH <sub>2</sub> )
8	153.9 (qC)	152.9 (qC)	151.0 (qC)	156.4 (qC)	78.9 (qC)	79.6 (qC)	78.8 (qC)
9	42.7 (CH <sub>2</sub> )	42.2 (CH <sub>2</sub> )	43.2 (CH <sub>2</sub> )	42.4 (CH <sub>2</sub> )	46.5 (CH <sub>2</sub> )	41.7 (CH <sub>2</sub> )	41.5 (CH <sub>2</sub> )
10	83.0 (CH)	83.8 (CH)	83.2 (CH)	79.7 (CH)	78.1 (CH)	79.1 (CH)	64.2 (CH)
11	71.4 (CH)	72.0 (CH)	71.8 (CH)	148.3 (CH)	149.1 (CH)	153.0 (CH)	62.7 (CH)
12	131.8 (qC)	131.5 (qC)	130.6 (qC)	134.9 (qC)	132.9 (qC)	130.5 (qC)	65.0 (qC)
13	147.4 (CH)	147.4 (CH)	145.0 (CH)	21.4 (CH <sub>2</sub> )	19.8 (CH <sub>2</sub> )	66.9 (CH)	73.4 (CH)
14	27.2 (CH <sub>2</sub> )	30.8 (CH <sub>2</sub> )	29.9 (CH <sub>2</sub> )	30.3 (CH <sub>2</sub> )	25.9 (CH <sub>2</sub> )	39.3 (CH <sub>2</sub> )	34.3 (CH <sub>2</sub> )
15	145.4 (qC)	147.3 (qC)	144.5 (qC)	145.4 (qC)	146.5 (qC)	147.4 (qC)	148.3 (qC)
16	111.0 (CH <sub>2</sub> )	110.6 (CH <sub>2</sub> )	110.3 (CH <sub>2</sub> )	113.3 (CH <sub>2</sub> )	111.6 (CH <sub>2</sub> )	112.1 (CH <sub>2</sub> )	110.4 (CH <sub>2</sub> )
17	22.4 (CH <sub>3</sub> )	21.2 (CH <sub>3</sub> )	23.3 (CH <sub>3</sub> )	18.8 (CH <sub>3</sub> )	21.0 (CH <sub>3</sub> )	19.1 (CH <sub>3</sub> )	22.2 (CH <sub>3</sub> )
18	23.6 (CH <sub>3</sub> )	22.5 (CH <sub>3</sub> )	24.3 (CH <sub>3</sub> )	22.5 (CH <sub>3</sub> )	26.6 (CH <sub>3</sub> )	28.0 (CH <sub>3</sub> )	27.3 (CH <sub>3</sub> )
19	168.6 (qC)	167.5 (qC)	166.2 (qC)	173.0 (qC)	173.2 (qC)	172.8 (qC)	167.2 (qC)
5-OMe			58.1 (CH <sub>3</sub> )				
19-OMe							52.5 (CH <sub>3</sub> )

<sup>a</sup> Spectra were measured in CDCl<sub>3</sub> (100 MHz).<sup>b</sup> Spectra were measured in CDCl<sub>3</sub> (125 MHz).<sup>c</sup> Multiplicities are deduced by HSQC and DEPT experiments.

124.2 (CH, C-7), and 153.9 (qC, C-8) exhibited the presence of an  $\alpha,\beta$ -unsaturated ketone, which was further identified by a strong IR spectrum absorptions at 1667 cm<sup>-1</sup>. Two secondary hydroxyls were recognized as being present in **1** from its <sup>1</sup>H NMR signals at  $\delta_{\text{H}}$  4.36 (1H, dd, *J* = 6.0, 2.0 Hz, H-5) and 4.60 (1H, s, H-11), <sup>13</sup>C NMR signals at  $\delta_{\text{C}}$  74.1 (CH, C-5) and 71.4 (CH, C-11), as well as a broad IR absorption at 3418 cm<sup>-1</sup>. Moreover, the NMR signals [ $\delta_{\text{H}}$  4.42 (1H, s, H-16a) and 4.85 (1H, s, H-16b);  $\delta_{\text{C}}$  145.4 (qC, C-15) and 111.0 (CH<sub>2</sub>, C-16)] assigned a 1,1-disubstituted double bond in **1**. The above functionalities also account for seven of the eight degrees of unsaturation, suggesting a macrocyclic 14-membered ring in **1**.

By interpretation of <sup>1</sup>H–<sup>1</sup>H COSY correlations, it was possible to establish four partial structures of consecutive proton systems extending from H<sub>2</sub>-2 to H-13 through H-1 and H<sub>2</sub>-14, from H<sub>2</sub>-4 to H-5, and from H<sub>2</sub>-9 to H-10, as well as long-range COSY correlations between H<sub>2</sub>-16/H<sub>3</sub>-17, H<sub>3</sub>-18/H-7, and H<sub>2</sub>-9/H-7 (Fig. 1).

Moreover, the long-range <sup>1</sup>H–<sup>13</sup>C correlations observed from H<sub>2</sub>-16 to C-1 and C-17; from H<sub>3</sub>-17 to C-1, C-15, and C-16; from H<sub>2</sub>-2 to C-1, C-3, C-14, and C-15; from H<sub>2</sub>-14 to C-1, C-2, C-12, and C-13; from H-13 to C-11; from H-11 to C-9, C-10, C-13, and C-19; from H<sub>3</sub>-18 to C-7, C-8, and C-9; from H-7 to C-6, C-9, and C-18; from H<sub>2</sub>-4 to C-3, C-5, and C-6 led the connectivities of these partial structures (Fig. 1). Accordingly, the planar structure of gyro-sanolide A (**1**) was determined unambiguously.

The relative stereochemistry of **1** assigned by NOESY spectrum was compatible with those of **1** offered by computer modeling, in which the close contacts of atoms calculated in space were consistent with the NOESY correlations (Fig. 2). The NOESY correlations between H-7/H-9b ( $\delta_{\text{H}}$  2.87), H<sub>3</sub>-18/H-9a ( $\delta_{\text{H}}$  2.56), and H-11/H-13 indicated that the geometries of the two double bonds at C-7/C-8 and C-12/C-13 were assigned as *E* and *Z*, respectively. The absence of NOESY correlation between H-7 and H-11 suggested the *s-trans* geometry of the conjugated enone. The relative configurations of

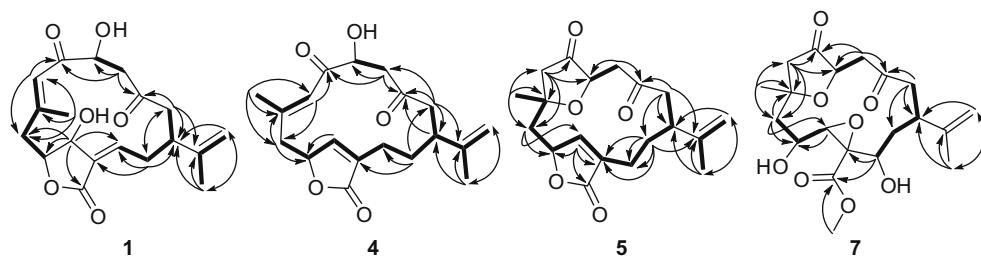


Figure 1. Selected  $^1\text{H}$ – $^1\text{H}$  COSY (–) and HMBC (→) correlations of **1**, **4**, **5**, and **7**.

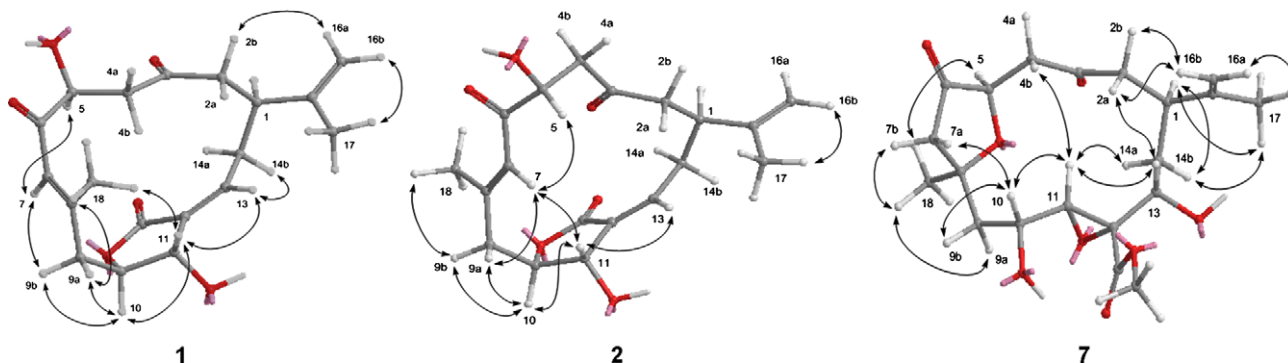


Figure 2. Key NOESY correlations and computer-generated perspective model using MM2 force field calculations for **1**, **2**, and **7**.

C-1, C-5, C-10, and C-11 in **1** were elucidated as  $1S^*$ ,  $5S^*$ ,  $10R^*$ , and  $11R^*$  by the following NOESY correlations between H-1/H-14a ( $\delta_{\text{H}}$  2.22), H-14b ( $\delta_{\text{H}}$  3.53)/H-13, H-13/H-11, H-11/H<sub>3</sub>-18, H<sub>3</sub>-18/H-9a, H-10/H-9a, H-10/H-9b, H-11/H-9b, and H-7/H-5, as shown in a computer generated 3D drawing. Thus, gyrosanolide A (**1**) was unambiguously formulated as  $(1S^*, 5S^*, 10R^*, 11R^*, 7E, 12Z)$ -5,11-dihydroxy-1-isopropenyl-3,6-dioxocyclotetradec-7,12,15(16)-trien-10,12-carbolactone.

The molecular formula of **2** was identical to that of **1** as indicated by HRESIMS. Comprehensive analysis of 2D NMR data, including the results of  $^1\text{H}$ – $^1\text{H}$  COSY, HMQC, and HMBC experiments, enabled the complete planar structure of gyrosanolide B to be assigned, as in **1**, to a C-4 norcembranoid skeleton. Comparison of the overall NMR spectroscopic data (Tables 1 and 2) indicated that **1** and **2** were isomers and exhibited significant variations in the  $^1\text{H}$  NMR chemical shifts for H-7 and H<sub>3</sub>-18. Furthermore, the crucial NOESY correlations (Fig. 2) between H-7 and H-11 proved the *s-cis* geometry of the conjugated enone. Additionally, the calculated torsion angle formed by C=O, C-6, C-7, and C-18 is  $19.8^\circ$ , further suggesting that the *s-cis* conformation of the conjugated enone moiety.<sup>16</sup> The key NOESY correlations between H-1/H<sub>2</sub>-2, H-1/H-17, H-16a ( $\delta_{\text{H}}$  4.72)/H-2a ( $\delta_{\text{H}}$  2.38), H-13/H-11, H-11/H-10, H-11/H<sub>3</sub>-18, H-7/H-5, H-10/H<sub>2</sub>-9, H<sub>3</sub>-18/H-9b ( $\delta_{\text{H}}$  2.87), H-7/H-9a ( $\delta_{\text{H}}$  2.48) indicated that **2** possessed the same relative configurations as **1** at the C-1, C-5, C-10, and C-11 stereocenters. Based on the aforementioned findings, it was concluded that gyrosanolide B (**2**) was a geometric isomer of **1**.

Gyrosanolide C (**3**) gave a formula of  $\text{C}_{20}\text{H}_{26}\text{O}_6$ , from the interpretation of its HRESIMS and  $^{13}\text{C}$  NMR spectroscopic data (Table 2). The complete analysis of COSY, HMBC, and HSQC spectra permitted us to assign all the spectroscopic signals and to propose the planar structure for **3**. The NMR features (Tables 1 and 2) of **3** were analogous to those of **2** with the exception that the resonances due to the secondary hydroxyl at C-5 [ $\delta_{\text{H}}$  4.29 (1H, t,  $J = 4.0$  Hz) and  $\delta_{\text{C}}$  72.4 (CH)] were replaced by those due to a

methoxyl [ $\delta_{\text{H}}$  3.90 (1H, dd,  $J = 7.6, 2.8$  Hz) and 3.41 (3H, s);  $\delta_{\text{C}}$  82.4 (CH), and 58.1 (CH<sub>3</sub>)]. The HMBC correlation (Fig. 1) from 5-OMe to C-5 indicated that the position of the methoxy group at C-5. Moreover, H-7 exhibited a NOESY correlation with 5-OMe, but did not show a NOESY correlation with H-5. The relative configuration of C-5 was assumed to be  $R^*$  according to the above NOESY correlations. Based on the similarity of the others NOESY correlations, the relative configurations at C-1, C-10, and C-11 of **3** were assumed to be identical with those of **2**. Therefore, the structure of gyrosanolide C (**3**) was definitively established as  $(1S^*, 5R^*, 10R^*, 11R^*, 7E, 12Z)$ -11-hydroxy-1-isopropenyl-5-methoxy-3,6-dioxocyclotetradec-7,12,15(16)-trien-10,12-carbolactone.

Gyrosanolide D (**4**) was isolated as a colorless oil, which analyzed for the molecular formula  $\text{C}_{19}\text{H}_{24}\text{O}_5$  by HRESIMS coupled with the DEPT and  $^{13}\text{C}$  NMR spectroscopic data (Table 2), indicating the existence of eight degrees of unsaturation. The IR spectrum exhibited the presence of conjugated ketone ( $1699\text{ cm}^{-1}$ ),  $\alpha,\beta$ -unsaturated  $\gamma$ -lactone ( $1745\text{ cm}^{-1}$ ) and hydroxy ( $3429\text{ cm}^{-1}$ ) functionalities. The  $^{13}\text{C}$  NMR spectrum showed signals of 19 carbons differentiated by DEPT into two methyls, five methylenes, six methines, and six quaternary carbons. The carbon resonances at  $\delta_{\text{C}}$  79.7 (CH, C-10), 148.3 (CH, C-11), 134.9 (CH, C-12), and 173.0 (qC, C-19) were assigned to the  $\alpha,\beta$ -unsaturated  $\gamma$ -lactone moiety, which was further supported by the deshielded olefinic proton at  $\delta_{\text{H}}$  7.06 (1H, s, H-11). The signals appearing at  $\delta_{\text{C}}$  206.9 (qC, C-3) and 200.1 (qC, C-6) were attributable to carbons of a normal ketone and  $\alpha,\beta$ -conjugated ketone. Furthermore, the six carbon signals appearing at  $\delta_{\text{C}}$  124.4 (CH, C-7) and 156.4 (qC, C-8), 148.3 (CH, C-11) and 134.9 (qC, C-12), and 145.4 (qC, C-15) and 113.3 (CH<sub>2</sub>, C-16) designated the presence of a trisubstituted double bond, a terminal double bond, and an oxymethine, respectively. Comparison of the NMR spectroscopic data of **4** with those of **11**,<sup>8</sup> it was suggested that **4** had the same norcembrane carbon skeleton as that of **11** but with an additional trisubstituted double bond at C-7 and C-8. The location of this double bond was established by the HMBC correla-

tions from H<sub>3</sub>-18/ H<sub>2</sub>-9 to C-7 and C-8, respectively. The relative configuration of **4** was determined through inspection of the NOESY spectrum as well as a computer-generated lower energy conformation using MM2 force field calculations. The relative configuration of C-5 was assumed to be *R*\* according to the absence of the crucial NOESY correlation between H-7 and H-5. By the assistance of COSY, NOESY, HMQC and HMBC experiments, **4** was surely deduced as (1*S*\*,5*R*\*,10*R*\*,7*E*,11*Z*)-5-hydroxy-1-isopropenyl-3,6-dioxocyclotetradec-7,11,15(17)-trien-10,12-carbolactone.

(1*S*\*,5*R*\*,8*S*\*,10*S*\*,11*Z*)-5,8-epoxy-1-isopropenyl-8-methyl-3,6-dioxocyclotetradec-11,15(16)-dien-10,12-carbolactone (**5**) was assigned a molecular formula of C<sub>19</sub>H<sub>24</sub>O<sub>5</sub>, according to its HRESIMS and NMR spectroscopic data (Tables 2 and 3). By interpretation of

<sup>1</sup>H-<sup>1</sup>H COSY correlations (Fig. 1), it was possible to establish three partial structures of consecutive proton systems extending from H<sub>2</sub>-2 to H<sub>2</sub>-13 through H-1, H<sub>2</sub>-14, and H<sub>2</sub>-13; from H<sub>2</sub>-4 to H-5; from H<sub>2</sub>-9 to H-11 through H-10, as well as long-range COSY correlations between H<sub>2</sub>-16/H<sub>3</sub>-17, H<sub>3</sub>-18/H-9, and H<sub>2</sub>-13/H-11. The HMBC correlations (Fig. 1) from H<sub>2</sub>-16 to C-1, C-17; from H<sub>3</sub>-17 to C-1, C-15, and C-16; from H<sub>2</sub>-2 to C-1, C-3, C-14, and C-15; from H<sub>2</sub>-14 to C-12, C-13, and C-15; from H-13 to C-11 and C-12; from H-11 to C-10, C-12, and C-19; from H<sub>2</sub>-9 to C-10, C-11, and C-18; from H<sub>3</sub>-18 to C-7, C-8, and C-9; from H-7 to C-5 C-6, C-8, C-9, and C-18; from H<sub>2</sub>-4 to C-3 and C-5 revealed the connectivity of the above partial structures. Thus, compound **5** was established to have the same planar structure as **10**, which was isolated from

**Table 3**

<sup>1</sup>H NMR spectroscopic data of compounds **4**–**7**

H#	<b>4</b> <sup>a</sup>	<b>5</b> <sup>b</sup>	<b>6</b> <sup>b</sup>	<b>7</b> <sup>b</sup>
1	1.96 m	2.75 m	2.77 m	2.95 m
2	a: 2.24 dd (13.0, 7.5) <sup>c</sup> b: 2.50 dd (12.5, 4.5)	a: 2.35 dd (16.8, 10.0) <sup>c</sup> b: 2.44 dd (16.8, 2.8)	a: 2.47 m b: 2.52 m	a: 2.78 m b: 2.50 dd (13.6, 4.8) <sup>c</sup>
4	a: 2.76 dd (18.5, 4.0) b: 2.87 dd (18.5, 8.5)	a: 2.57 dd (17.2, 9.6) b: 2.79 dd (17.2, 3.2)	2.58 m	a: 3.01 dd (16.8, 3.2) b: 2.71 m
5	4.65 m	4.54 dd (10.0, 3.2)	4.24 dd (8.8, 4.0) <sup>c</sup>	4.29 br dd (7.2, 3.2)
7	5.96 s	a: 2.53 d (18.4) b: 2.65 d (18.4)	a: 2.43 d (17.2) b: 2.54 d (17.6)	a: 2.69 d (18.0) b: 2.35 d (18.0)
9	a: 2.63 dd (13.5, 3.0) b: 2.97 dd (13.5, 5.5)	a: 1.72 dd (14.0, 10.4) b: 2.45 dd (14.0, 5.2)	a: 2.27 dd (15.2, 2.8) b: 2.64 dd (15.2, 4.4)	a: 2.20 m b: 2.18 m
10	5.24 m	5.09 m	5.28 br s	4.37 ddd (10.8, 5.2, 2.0)
11	7.06 s	7.44 d (1.6)	7.36 s	3.33 d (2.0)
13	2.31 m	a: 2.14 m b: 2.35 dd (16.8, 10.0)	4.73 br s	3.52 br d (6.4)
14	a: 1.70 m b: 1.82 m	a: 1.81 ddd (14.4, 9.6, 4.0) b: 1.98 m	a: 1.91 m b: 2.35 m	a: 2.18 m b: 2.15 m
16	a: 4.68 s b: 4.83 s	a: 4.70 s b: 4.87 s	a: 4.76 s b: 4.80 s	a: 4.87 s b: 4.74 s
17	1.67 s	1.75 s	1.76 s	1.87 s
18	2.20 s	1.51 s	1.48 s	1.35 s
19-OMe				3.80 s

<sup>a</sup> Spectra were measured in CDCl<sub>3</sub> (500 MHz).

<sup>b</sup> Spectra were measured in CDCl<sub>3</sub> (400 MHz).

<sup>c</sup> *J* values (in Hz) are in parentheses.

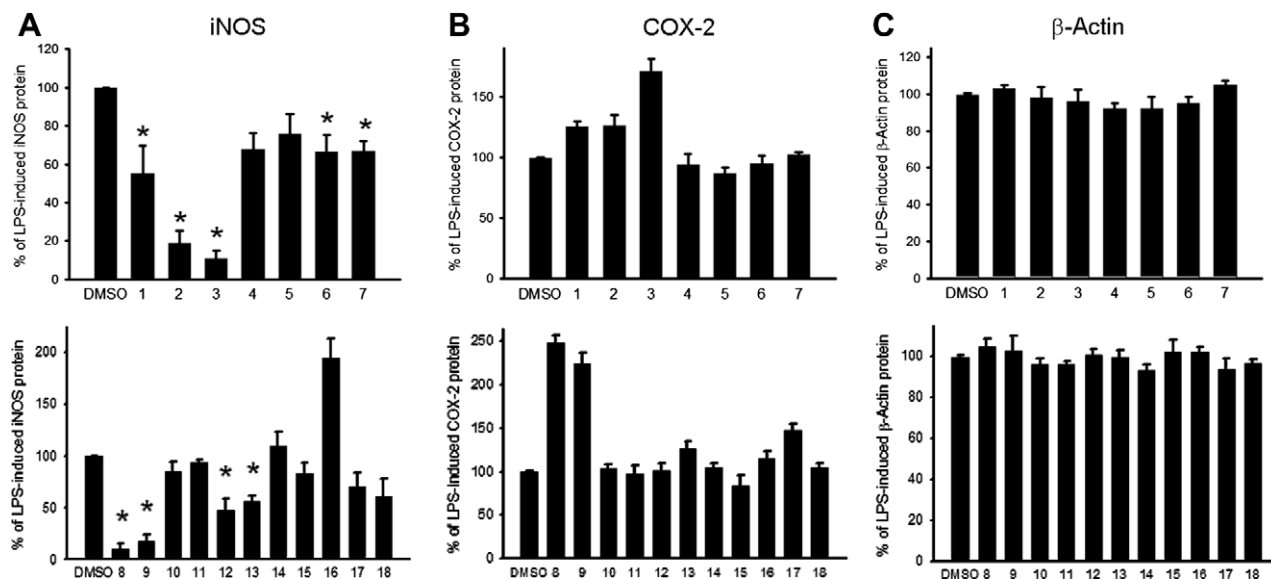
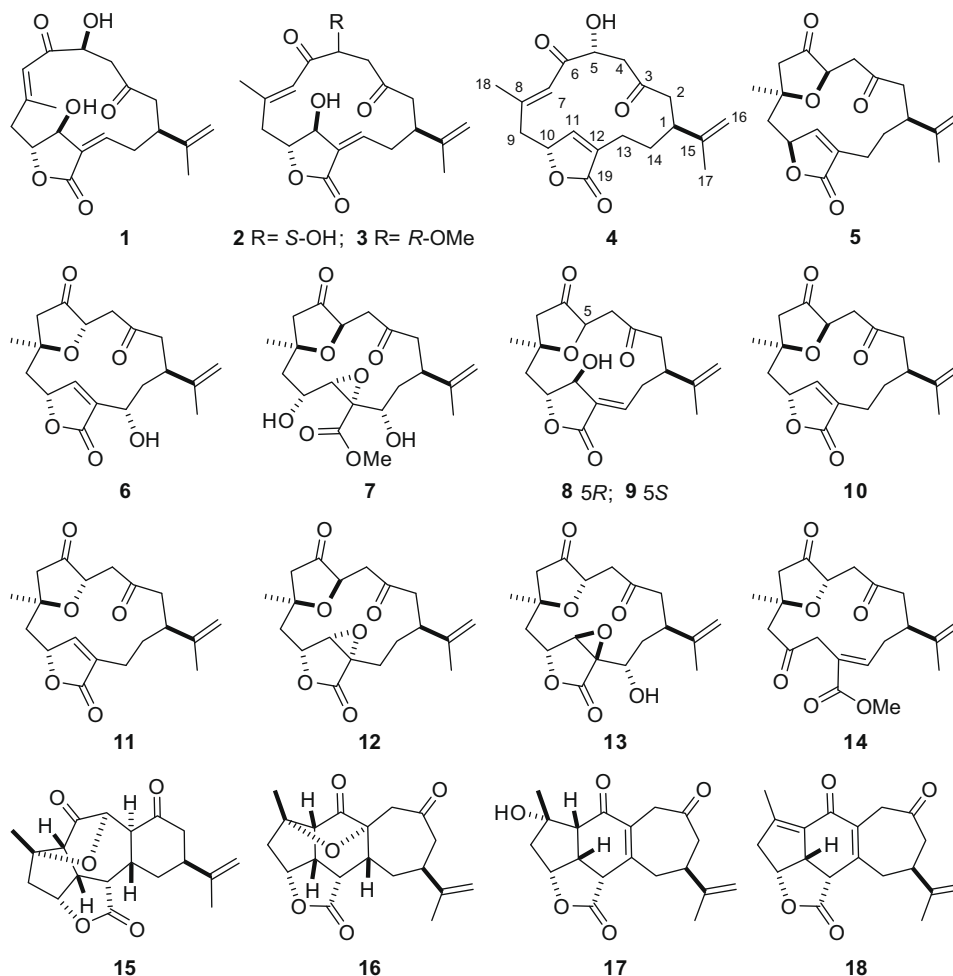


**Figure 3.** Effect of compounds **1**–**18** at 10  $\mu$ M on the LPS-induced pro-inflammatory iNOS and COX-2 protein expression of RAW 264.7 macrophages by immunoblot analysis. (A) Immunoblot of iNOS; (B) Immunoblot of COX-2; (C) Immunoblot of  $\beta$ -actin. The values are mean  $\pm$  SEM ( $n = 5$ ). The relative intensity of the LPS alone stimulated group was taken as 100%. \*Significantly different from LPS-stimulated (control) group ( $P < 0.05$ ).

the soft coral *Syntrophomonas erecta*.<sup>8</sup> The signal at  $\delta_{\text{H}}$  5.09 (1H, m, H-10) showed NOESY correlations with  $\delta_{\text{H}}$  7.44 (1H, d,  $J = 1.6$  Hz, H-11) and 1.51 (3H, s, H-18), suggesting the  $S^*$  configuration at C-10 of **5**. Meanwhile, a crucial NOESY correlation between H<sub>3</sub>-18 and H-10 (not existing in **10**), and chemical shift changes of H-10, H-11, and H<sub>3</sub>-18 ( $\delta_{\text{H}}$  5.14, 7.22, and 1.32, respectively in CDCl<sub>3</sub> of **10**) indicated that gyrosanolide E (**5**) is the 10-epimer of **10**.

The HRESIMS and NMR spectroscopic data (Tables 2 and 3) gave the molecular formula of **6** as C<sub>19</sub>H<sub>24</sub>O<sub>6</sub>, which was 16 amu greater than that of **11**.<sup>8</sup> A comparison of the NMR and IR data revealed that **6** differed from **12** solely due to the substitution at C-13, where a hydroxymethine [ $\delta_{\text{H}}$  4.73 (1H, br s) and  $\delta_{\text{C}}$  66.9 (CH)] of **6** replaced a methylene [ $\delta_{\text{H}}$  2.18 (1H, m) and 2.40 (1H, m);  $\delta_{\text{C}}$  20.0 (CH<sub>2</sub>)] of the latter. The NOESY experiment revealed that **6** possessed the same configurations at C-1, C-5, C-8 and C-10 as in **11**. Furthermore, one of the C-2 methylene protons, H-2a ( $\delta_{\text{H}}$  2.47, m), showed a NOESY correlation with H-1, while the other H-2b ( $\delta_{\text{H}}$  2.52, m) was correlated with H-13. The above result indicated that the hydroxy group at C-13 should be demonstrated the  $S^*$  configuration. Hence, gyrosanolide F (**6**) was unequivocally elucidated as (1 $S^*$ ,5 $S^*$ ,8 $S^*$ ,10 $R^*$ ,13 $S^*$ ,11 $Z$ )-5,8-epoxy-13-hydroxy-1-isopropenyl-8-methyl-3,6-dioxocyclotetradec-11,15(16)-dien-10,12-carbolactone.

Compound **7** analyzed for C<sub>20</sub>H<sub>28</sub>O<sub>8</sub> from HRESIMS ( $m/z$  419.1684, [M+Na]<sup>+</sup>) and <sup>13</sup>C NMR spectroscopic data (Table 2), indicating seven degrees of unsaturation. The IR spectrum of **7** at 3485 cm<sup>-1</sup> demonstrated a broad absorption band diagnostic of secondary hydroxyls, which were further identified by the <sup>1</sup>H NMR signals at  $\delta_{\text{H}}$  4.37 (1H, ddd,  $J = 10.8, 5.2, 2.0$  Hz, H-10) and 3.52 (1H, br d,  $J = 6.4$  Hz, H-13), and <sup>13</sup>C NMR signals at  $\delta_{\text{C}}$  64.2 (CH, C-10) and 73.4 (CH, C-13). The NMR spectroscopic data (Tables 2 and 3) indicated that **7** possesses a 1,1-disubstituted olefins [ $\delta_{\text{H}}$  4.87 (1H, s, H-16a) and 4.74 (1H, s, H-16b);  $\delta_{\text{C}}$  148.3 (qC, C-15) and 110.4 (CH<sub>2</sub>, C-16)], a trisubstituted epoxide [ $\delta_{\text{H}}$  3.33 (1H, d,  $J = 2.0$  Hz, H-11);  $\delta_{\text{C}}$  62.7 (CH, C-11) and 65.0 (qC, C-12)], and a methyl ester [ $\delta_{\text{H}}$  3.80 (3H, s, 19-OMe);  $\delta_{\text{C}}$  167.2 (qC, C-19) and 52.5 (CH<sub>3</sub>, 19-OMe)]. The carbon resonances appearing at  $\delta_{\text{C}}$  208.4 (qC, C-3) and 214.2 (qC, C-6) were attributable to carbons of two normal ketones. Although there were no direct HMBC correlations available, the remaining one unsaturation indicated that an oxygen bridge is probably present between one oxygenated methine [ $\delta_{\text{H}}$  4.29 (dd, 1H,  $J = 7.2, 3.2$  Hz, H-5) and  $\delta_{\text{C}}$  75.4 (CH, C-5)] and an oxygenated quaternary carbon [ $\delta_{\text{C}}$  78.8 (qC, C-8)]. This assumption was further supported by the NOESY correlation between H-5 and H<sub>3</sub>-18 (Fig. 2). The above functionalities account for six of the seven degrees of unsaturation, suggesting that **7** must consist of a macrocyclic 14-membered ring.





Correlations deduced from extensive analysis of the  $^1\text{H}$ – $^1\text{H}$  COSY correlations of **7** enabled initially the establishment of three partial structures. The connectivity of the above structural fragments was subsequently interconnected by the crucial HMBC correlations (Fig. 1). The computer-modeled structure of **7** was generated by CS Chem 3D version 11.0 using MM2 force field calculations for energy minimization (Fig. 2). The result was consistent with the relative stereochemistry of **7** as established mainly by the assistance of the NOESY experiment. The NOE correlations between H-7a ( $\delta_{\text{H}}$  2.69)/H-10, H-10/H-9b ( $\delta_{\text{H}}$  2.18), H-11/H-4b ( $\delta_{\text{H}}$  2.71), H-10/H-11, H-11/H-13, H-11/H-14a ( $\delta_{\text{H}}$  2.18), H-13/H-2a ( $\delta_{\text{H}}$  2.78), H-1/H-14b ( $\delta_{\text{H}}$  2.15), H<sub>3</sub>-17/H-16a ( $\delta_{\text{H}}$  4.87), H-1/H<sub>3</sub>-17, H-16b ( $\delta_{\text{H}}$  4.74)/H-2a, H-16b/H-2b ( $\delta_{\text{H}}$  2.50), H-9a ( $\delta_{\text{H}}$  2.20)/H<sub>3</sub>-18, H-7b ( $\delta_{\text{H}}$  2.35)/H<sub>3</sub>-18, and H-5/H<sub>3</sub>-18 demonstrated the 1S\*, 5R\*, 8S\*, 10R\*, 11S\*, 12S\*, and 13S\* configurations as depicted in Figure 2. Therefore, gyrosanolide **7** (**7**) was fully determined as methyl (1S\*,5R\*,8S\*,10R\*,11S\*,12S\*,13S\*)-5,8,11,12-diepoxy-10,13-dihydroxy-1-isopropenyl-8-methyl-3,6-dioxocyclotetradec-15(16)-en-19-carboxylate.

Compounds **1**–**18** were tested for their cytotoxicity against the P-388, A-459, and HT-29 cancer cell lines. Preliminary cytotoxic screening revealed that **7** displayed cytotoxicity against P-388 cell line with an ED<sub>50</sub> value of 3.6  $\mu\text{g/mL}$ . However, the other tested compounds were not cytotoxic to P-388, A-549, and HT-29 cells (>20.0  $\mu\text{g/mL}$ ). The anticancer agent mithramycin was used as the positive control and exhibited ED<sub>50</sub> values of 0.06, 0.07, and 0.08  $\mu\text{g/mL}$  against P-388, A-549, and HT-29 cells, respectively.

At a concentration of 1  $\mu\text{g/mL}$ , compound **8** showed significant antiviral activity against HCMV cells with an IC<sub>50</sub> value of 1.9  $\mu\text{g/mL}$ . With the exception of the above findings, the obtained negative results showed that the others exhibited no discernible activity against HCMV cells (ED<sub>50</sub> >50  $\mu\text{g/mL}$ ). In addition, the antibacterial activity assays revealed that none of compounds exhibited any antibacterial activity against *E. aerogenes*, *S. enteritidis*, *S. marcescens*, *S. sonnei*, and *Y. enterocolitica* at a concentration of 100  $\mu\text{g/disk}$ .

Our previous studies have reported that cembrane-type diterpenoids possess iNOS and COX-2 proteins inhibition,<sup>17–19</sup> which prompted us to evaluate the anti-inflammatory effect of these isolated compounds **1**–**18**. Stimulation of RAW 264.7 cells with LPS resulted in up-regulation of the pro-inflammatory iNOS and COX-2 proteins (Fig. 3). Compounds **1**–**3**, **7**–**9**, **12**, and **13** at concentration of 10  $\mu\text{M}$  did not inhibit the COX-2 protein expression, but significantly reduced the levels of the iNOS protein (55.2  $\pm$  14.6%, 18.6  $\pm$  6.7%, 10.6  $\pm$  4.6%, 66.9  $\pm$  5.2%, 10.2  $\pm$  5.1%, 17.4  $\pm$  7.2%, 47.2  $\pm$  11.9%, and 56.3  $\pm$  5.1%, respectively) by LPS stimulation. Moreover, the house keeping protein  $\beta$ -actin was not changed by the presence of these tested compounds at the same concentration. Under the same experimental condition, 10  $\mu\text{M}$  CAPE (caffeic acid phenylthyl ester; Sigma Chemical Company, St. Louis, MO) reduced the levels of the iNOS and COX-2 protein to 1.5  $\pm$  2.1% and 70.2  $\pm$  11.5%, respectively, relative to the control cells stimulated with LPS. Compounds **3**, **8** and **9** were significantly increased pro-inflammatory protein, COX-2 level in LPS-stimulated macrophage.

### 3. Experimental

#### 3.1. General experimental procedures

Optical rotations were determined with a JASCO P1020 digital polarimeter. Ultraviolet (UV) and infrared (IR) spectra were obtained on a JASCO V-650 and JASCO FT/IR-4100 spectrometer, respectively. The NMR spectra were recorded on a Varian MR 400 NMR spectrometer at 400 MHz for  $^1\text{H}$  and 100 MHz for  $^{13}\text{C}$  or on a Varian Unity INOVA 500 FT-NMR spectrometer at

500 MHz for  $^1\text{H}$  and 125 MHz for  $^{13}\text{C}$ , respectively. Chemical shifts are expressed in  $\delta$  (ppm) referring to the solvent peaks  $\delta_{\text{H}}$  7.27 and  $\delta_{\text{C}}$  77.0 for  $\text{CDCl}_3$ , respectively, and coupling constants are expressed in Hz. ESIMS were recorded by ESI FT-MS on a Bruker APEX II mass spectrometer. Silica Gel 60 (Merck, 230–400 mesh) and LiChroprep RP-18 (Merck, 40–63  $\mu\text{m}$ ) were used for column chromatography. Precoated silica gel plates (Merck, Kieselgel 60 F<sub>254</sub>, 0.25 mm) and precoated RP-18 F<sub>254s</sub> plates (Merck, 1.05560) were used for analytical TLC analyses. High-performance liquid chromatography (HPLC) was carried out using a Hitachi L-7100 pump equipped with a Hitachi L-7400 UV detector at 220 nm and a semi-preparative reversed phase column (Merck, Hibar Purospher RP-18e, 5  $\mu\text{m}$ , 250  $\times$  10 mm).

#### 3.2. Animal materials

The soft coral *S. gyrosa* was collected by hand using scuba techniques at the Dongsha Atoll off Taiwan, in April 2007, at a depth of 8–10 m, and was stored in a freezer for two months until extraction. This soft coral was identified by one of the authors (C.-F.D.). A voucher specimen (TS-19) was deposited in the Department of Marine Biotechnology and Resources, National Sun Yat-sen University.

#### 3.3. Extraction and isolation

The frozen specimen of *S. gyrosa* (2.0 kg) was chopped into small pieces and extracted with fresh acetone for 24 h at room temperature. The quantity of solvent used for each extraction (2.0 L) was at least three times the amount of the soft coral material used. The combined acetone extracts were concentrated to a brown gum, which was partitioned between  $\text{H}_2\text{O}$  and EtOAc. The resulting EtOAc partition (30.0 g) was subjected to column chromatography on silica gel using *n*-hexane–EtOAc and EtOAc–MeOH mixtures of increasing polarity for elution to furnish 40 fractions. Fraction 20 (0.48 g) eluted with *n*-hexane–EtOAc (1:10) was subjected to column chromatography on silica gel using *n*-hexane–EtOAc mixtures of increasing polarity for elution to give 12 subfractions. A subfraction 20-6 (161 mg) eluted with *n*-hexane–EtOAc (2:1) was further subjected to column chromatography on silica gel using *n*-hexane–EtOAc (2:1) for elution to separate 11 subfractions. Then, the subfraction 20-6-6 (45 mg) was purified by RP-18 HPLC using MeOH– $\text{H}_2\text{O}$  (53:47) to afford **10** (2 mg), **11** (3 mg), **12** (4 mg), and **18** (2 mg). Similarly, subfractions 20-6-7 (49 mg) and 20-6-11 (16 mg) were further purified by RP-HPLC using MeOH– $\text{H}_2\text{O}$  (53:47) to afford **5** (1 mg) and **15** (3 mg). Fraction 22 (1.50 g) eluted with EtOAc–MeOH (90:1) was subjected to a silica gel column using *n*-hexane–EtOAc gradient (4:1–0:100) for elution to give 12 subfractions. In turn, a subfraction 22-4 (378 mg) eluted with *n*-hexane–EtOAc (1:4) was chromatographed on a silica gel column using *n*-hexane–EtOAc (1:3) for elution to separate 8 subfractions. Subsequently, a subfraction 22-4-3 (115 mg) was purified by RP-18 HPLC using MeOH– $\text{H}_2\text{O}$  (45:55) to afford **3** (1 mg), **8** (28 mg), **9** (51 mg), **13** (3 mg), **16** (1 mg), and **17** (1 mg), respectively. Fraction 30 (0.16 g) eluted with EtOAc–MeOH (10:1) was applied to column chromatography on a RP-18 gel column eluting with 45% MeOH in  $\text{H}_2\text{O}$  to provide a mixture that was further separated by RP-18HPLC using 45% MeOH in  $\text{H}_2\text{O}$  to provide **14** (8 mg) and a mixture. Then, the mixture was purified by column chromatography using *n*-hexane–EtOAc (1:5) to give **6** (3 mg). Fraction 33 (0.30 g) eluted with EtOAc–MeOH (4:1) was subjected to a silica gel column using EtOAc–MeOH (40:1) for elution, to separate 9 subfractions. A subfraction 33-3 (31 mg) was applied to column chromatography on a RP-18 gel column eluting with 45% MeOH in  $\text{H}_2\text{O}$  to afford a mixture that was further sepa-

rated by RP-18 HPLC using MeOH–H<sub>2</sub>O (45:55) to give **1** (3 mg), **2** (5 mg), **4** (1 mg), and **7** (1 mg).

### 3.3.1. Gyrosanolide A (1)

Colorless, viscous oil;  $[\alpha]_D^{25}$  –72 (c 0.1, CHCl<sub>3</sub>); UV (MeOH)  $\lambda_{\max}$  (log  $\epsilon$ ) 223 (3.69) nm; IR (KBr)  $\nu_{\max}$  3418, 2920, 1734, 1718, 1667, 1643, 1373, 1183, 1073 cm<sup>–1</sup>; <sup>1</sup>H NMR and <sup>13</sup>C NMR data, see Tables 1 and 2; ESIMS  $m/z$  371 [M+Na]<sup>+</sup>; HRESIMS  $m/z$  371.1472 [M+Na]<sup>+</sup> (calcd for C<sub>19</sub>H<sub>24</sub>O<sub>6</sub>Na, 371.1471).

### 3.3.2. Gyrosanolide B (2)

Colorless, viscous oil;  $[\alpha]_D^{25}$  –64.0 (c 0.1, CHCl<sub>3</sub>); UV (MeOH)  $\lambda_{\max}$  (log  $\epsilon$ ) 225 (3.88) nm; IR (KBr)  $\nu_{\max}$  3422, 2922, 2855, 1738, 1701, 1622, 1418, 1375, 1178, 1077 cm<sup>–1</sup>; <sup>1</sup>H NMR and <sup>13</sup>C NMR data, Tables 1 and 2; ESIMS  $m/z$  371 [M+Na]<sup>+</sup>; HRESIMS  $m/z$  371.1472 [M+Na]<sup>+</sup> (calcd for C<sub>19</sub>H<sub>24</sub>O<sub>6</sub>Na, 371.1471).

### 3.3.3. Gyrosanolide C (3)

Colorless, viscous oil;  $[\alpha]_D^{25}$  –78 (c 0.1, CHCl<sub>3</sub>); UV (MeOH)  $\lambda_{\max}$  (log  $\epsilon$ ) 226 (3.97) nm; IR (KBr)  $\nu_{\max}$  3425, 2924, 2852, 1745, 1696, 1643, 1616, 1376, 1179, 1095, 1034, 893, 734 cm<sup>–1</sup>; <sup>1</sup>H NMR and <sup>13</sup>C NMR data, see Tables 1 and 2; ESIMS  $m/z$  385 [M+Na]<sup>+</sup>; HRESIMS  $m/z$  385.1625 [M+Na]<sup>+</sup> (calcd for C<sub>20</sub>H<sub>26</sub>O<sub>6</sub>Na, 385.1627).

### 3.3.4. Gyrosanolide D (4)

Colorless, viscous oil;  $[\alpha]_D^{25}$  –96 (c 0.1, CHCl<sub>3</sub>); UV (MeOH)  $\lambda_{\max}$  (log  $\epsilon$ ) 218 (3.75), 242 (3.52) nm; IR (KBr)  $\nu_{\max}$  3429, 2924, 2852, 1745, 1699, 1639, 1407, 1206, 1087, 893 cm<sup>–1</sup>; <sup>1</sup>H NMR and <sup>13</sup>C NMR data, see Tables 2 and 3; ESIMS  $m/z$  355 [M+Na]<sup>+</sup>; HRESIMS  $m/z$  355.1525 [M+Na]<sup>+</sup> (calcd for C<sub>19</sub>H<sub>24</sub>O<sub>5</sub>Na, 355.1521).

### 3.3.5. Gyrosanolide E (5)

Colorless, viscous oil;  $[\alpha]_D^{25}$  –110 (c 0.1, CHCl<sub>3</sub>); UV (MeOH)  $\lambda_{\max}$  (log  $\epsilon$ ) 212 (3.97) nm; IR (KBr)  $\nu_{\max}$  3072, 2932, 1749, 1703, 1650, 1445, 1418, 1373, 1267, 1198, 1091, 1038, 893, 730 cm<sup>–1</sup>; <sup>1</sup>H NMR and <sup>13</sup>C NMR data, see Tables 2 and 3; ESIMS  $m/z$  355 [M+Na]<sup>+</sup>; HRESIMS  $m/z$  355.1519 [M+Na]<sup>+</sup> (calcd for C<sub>19</sub>H<sub>24</sub>O<sub>5</sub>Na, 355.1521).

### 3.3.6. Gyrosanolide F (6)

Colorless, viscous oil;  $[\alpha]_D^{25}$  –124 (c 0.1, CHCl<sub>3</sub>); UV (MeOH)  $\lambda_{\max}$  (log  $\epsilon$ ) 214 (3.77) nm; IR (KBr)  $\nu_{\max}$  3411, 3070, 2926, 2855, 1752, 1730, 1705, 1644, 1454, 1375, 1185, 1109, 1091, 1045, 897 cm<sup>–1</sup>; <sup>1</sup>H NMR and <sup>13</sup>C NMR data, see Tables 2 and 3; ESIMS  $m/z$  371 [M+Na]<sup>+</sup>; HRESIMS  $m/z$  371.1472 [M+Na]<sup>+</sup> (calcd for C<sub>19</sub>H<sub>24</sub>O<sub>6</sub>Na, 371.1471).

### 3.3.7. Gyrosanin A (7)

Colorless, viscous oil;  $[\alpha]_D^{25}$  –22 (c 0.1, CHCl<sub>3</sub>); IR (KBr)  $\nu_{\max}$  3485, 2956, 2923, 1737, 1709, 1645, 1435, 1374, 1246, 1096, 1049, 734 cm<sup>–1</sup>; <sup>1</sup>H NMR and <sup>13</sup>C NMR data, see Tables 2 and 3; ESIMS  $m/z$  419 [M+Na]<sup>+</sup>; HRESIMS  $m/z$  419.1684 [M+Na]<sup>+</sup> (calcd for C<sub>20</sub>H<sub>28</sub>O<sub>8</sub>Na, 419.1682).

## 3.4. In vitro cytotoxicity assay

Cytotoxicity was determined against P-388 (mouse lymphocytic leukemia), HT-29 (human colon adenocarcinoma), and A-549 (human lung epithelial carcinoma) tumor cells using a modification of the MTT colorimetric method. The provision of the P-388 cell line was supported by J. M. Pezzuto, formerly of the Department of Medicinal Chemistry and Pharmacognosy, University of Illinois at Chicago. These HT-29 and A-549 cell lines were purchased from the American Type Culture Collection. The experimental details of this assay were carried out according to a previously described procedure.<sup>20,21</sup>

## 3.5. In vitro antimicrobial activity

Bacterial strains were grown in LB (Luria-Bertani) broth medium for 24 h at 37 °C. Then, 17 mL LB hard agar (1.5% agar) was poured into sterile Petri dishes (9 cm) and allowed to set. Next, 2.7 mL molten LB soft agar (0.7% agar, 45 °C) was inoculated with 0.3 mL broth culture of the test organism and poured over the base hard agar plates forming a homogenous top layer. Sterile paper disks (Advantec, 8 mm) were placed onto the top layer of the LB agar plates. Ten microliters (2 µg/µL) of compounds **1–6** and **8–18** were applied on to each the filter paper disks. Ampicillin (5 µg/µL) and the same solvents were served as positive and negative controls. All plates were incubated at 37 °C, 24 h prior to antibacterial activity evaluation. The antimicrobial activity of the tested compounds was tested up to 100 µg/mL against *E. aerogenes* (ATCC13048), *S. enteritidis* (ATCC13076), *S. marcescens* (ATCC25419), *S. sonnei* (ATCC11060), and *Y. enterocolitica* (ATCC23715), respectively. All bacterial strains were obtained from the American Type Culture Collection. The antibiotic activity evaluation method was conducted based on previously reports.<sup>22,23</sup>

## 3.6. In vitro anti-inflammatory assay

Murine RAW 264.7 macrophages were obtained from the American Type Culture Collection (ATCC, No. TIB-71) and cultured in Dulbecco's modified essential medium (DMEM) containing 10% heat-inactivated fetal bovine serum, at 37 °C in a humidified 5% CO<sub>2</sub>–95% air incubator under standard conditions. The in vitro anti-inflammatory assay was carried out according to the procedure described previously.<sup>24,25</sup> For statistical analysis, all the data were analyzed by a one-way analysis of variance (ANOVA), followed by the Student–Newman–Keuls post hoc test for multiple comparisons. A significant difference was defined as a *P* value of <0.05.

## 3.7. Anti-cytomegalovirus assay

To determine the effects of natural product upon human cytomegalovirus (HCMV) cytopathic effect (CPE), confluent human embryonic lung (HEL) cells grown in 24-well plates will be incubated for 1 h in the presence or absence of various concentrations of tested natural product. Then, cells will be infected with HCMV at an input of 1000 pfu (plaque forming units) per well of 24-well dish. Antiviral activity is expressed as IC<sub>50</sub> (50% inhibitory concentration), or compound concentration required to reduce virus induced CPE by 50% after seven days as compared with the untreated control. To monitor the cell growth upon treating with natural products, an MTT-colorimetric assay was employed.<sup>26</sup>

## Acknowledgment

Financial supports were provided by National Science Council (NSC96-2320-B-110-003-MY3) of Taiwan awarded to C.-Y.D.

## References and notes

- Bowden, B. F.; Coll, J. C.; Mitchell, S. J.; Mulder, J.; Stokke, J. G. *Aust. J. Chem.* **1978**, *31*, 2049.
- Lakshmi, V.; Schmitz, F. J. *J. Nat. Prod.* **1986**, *49*, 728.
- Sato, A.; Fenical, W.; Zheng, Q.-T.; Clardy, J. *Tetrahedron* **1985**, *41*, 4303.
- Shoji, N.; Umeyama, A.; Arihara, S. *J. Nat. Prod.* **1993**, *56*, 1651.
- Iguchi, K.; Kajiyama, K.; Yamada, Y. *Tetrahedron Lett.* **1995**, *36*, 8807.
- Elsayed, K. A.; Hamann, M. T. *J. Nat. Prod.* **1996**, *59*, 687.
- Iguchi, K.; Kajiyama, K.; Miyaoka, H.; Yamada, Y. *J. Org. Chem.* **1996**, *61*, 5998.
- Rudi, A.; Dayan, T. L. A.; Aknin, M.; Gaydou, E. M.; Kashman, Y. *J. Nat. Prod.* **1998**, *61*, 872.
- Radhika, P.; Rao, P. V. S.; Anjaneyulu, V.; Asolkar, R. N.; Laatsch, H. *J. Nat. Prod.* **2002**, *65*, 737.
- Duh, C. Y.; Wang, S. K.; Chia, M. C. *Tetrahedron Lett.* **1999**, *40*, 6033.
- Sheu, J. H.; Ahmed, A. F.; Shiue, R. T.; Dai, C. F.; Kuo, Y. H. *J. Nat. Prod.* **2002**, *65*, 1904.

12. Ahmed, A. F.; Shiue, R. T.; Wang, G. H.; Dia, C. F.; Kuo, Y. H.; Sheu, J. H. *Tetrahedron* **2003**, 59, 7337.
13. Ahmed, A. F.; Su, J. H.; Kuo, Y. H.; Sheu, J. H. *J. Nat. Prod.* **2004**, 67, 2079.
14. Tseng, Y. J.; Ahmed, A. F.; Dia, C. F.; Chiang, M. Y.; Sheu, J. H. *Org. Lett.* **2005**, 7, 3813.
15. Rudi, A.; Shmul, G.; Benayahu, Y.; Kashman, Y. *Tetrahedron Lett.* **2006**, 47, 2937.
16. Liljefors, T.; Allinger, N. L. *J. Am. Chem. Soc.* **1976**, 98, 2745.
17. Cheng, S.-Y.; Wen, Z.-H.; Chiou, S.-F.; Wang, S.-K.; Hsu, C.-H.; Dai, C.-F.; Chiang, M. Y.; Duh, C.-Y. *Tetrahedron* **2008**, 64, 9698.
18. Cheng, S.-Y.; Wen, Z.-H.; Wang, S.-K.; Chiou, S.-F.; Hsu, C.-H.; Dai, C.-F.; Duh, C.-Y. *Bioorg. Med. Chem.* **2009**, 17, 3763.
19. Cheng, S.-Y.; Wen, Z.-H.; Wang, S.-K.; Chiou, S.-F.; Hsu, C.-H.; Dai, C.-F.; Chiang, M. Y.; Duh, C.-Y. *J. Nat. Prod.* **2009**, 72, 152.
20. Hou, R.-S.; Duh, C.-Y.; Chiang, M. Y.; Lin, C.-N. *J. Nat. Prod.* **1995**, 58, 1126.
21. Geran, R. I.; Greenberg, N. H.; MacDonald, M. M.; Schumacher, A. M.; Abbott, B. J. *Cancer Chemother. Rep.* **1972**, 3, 1.
22. Arias, M. E.; Gomez, J. D.; Cudmani, N. M.; Vattuone, M. A.; Isla, M. I. *Life Sci.* **2004**, 75, 191.
23. Hou, L.; Shi, Y.; Zhai, P.; Le, G. *J. Ethnopharmacol.* **2007**, 111, 227.
24. Jean, Y.-H.; Chen, W.-F.; Sung, C.-S.; Duh, C.-Y.; Huang, S.-Y.; Lin, C.-S.; Tai, M.-H.; Wen, Z.-H. *Br. J. Pharmacol.* **2009**, 158, 713.
25. Cheng, S.-Y.; Wen, Z.-H.; Wang, S.-K.; Chiang, M. Y.; El-Gamal, A. A. H.; Dai, C.-F.; Duh, C.-Y. *Chem. Biodivers.* **2009**, 6, 86.
26. Stevens, M.; Balzarini, J.; Tabarrini, O.; Andrei, G.; Snoeck, R.; Cecchetti, V.; Fravolini, A.; De Clercq, E.; Pannecouque, C. *J. Antimicrob. Chemother.* **2005**, 56, 847.